Membrane Formation with Presence of Lewis Acid–Base Complexes in Polymer Solution

CRISTINA C. PEREIRA, RONALDO NOBREGA, CRISTIANO P. BORGES

Chemical Engineering Program, COPPE/Federal University of Rio de Janeiro, P. O. Box 68.502, Rio de Janeiro, RJ 21945-970, Brazil

Received 22 November 1999; accepted 16 April 2001

ABSTRACT: This work investigated membrane formation using Lewis acid–base complexes in a polymer solution, which consisted of poly(ether sulfone) (PES), Lewis acid–base complexes formed by *N*-methyl-2-pyrrolidone (NMP, Lewis base), and dicarboxylic or monocarboxylic acids from a homologous series (Lewis acids). The solutions were characterized by viscosity measurements, IR spectroscopy, cloud point determination, and light transmission experiments. The membranes were characterized by scanning electron microscopy and gas permeation tests. The results indicated that the solvent–additive interaction, which is a function of their capacity to form complexes, and the acid chain length directly affect the viscosity and miscibility region. Consequently, these parameters combined with the complex dissociation influence the precipitation velocity of the polymer solutions, which will then affect the membrane transport properties. It is also pointed out that the membranes prepared by using 25 wt % PES at the same acid/NMP molar ratios and with different acids presented permeability coefficients in agreement with the binodal shift obtained in pseudoternary phase diagrams. Furthermore, when these solutions were exposed to the environment for a long period of time, the demixing onset sequence also agreed with the miscibility region for all solutions, except for the adipic acid solution because of its extremely high viscosity. J Appl Polym Sci 83: 2022–2034, 2002

Key words: membrane formation; poly(ether sulfone); Lewis acid–base complexes; gas separation

INTRODUCTION

Several research studies in the field of gas separation have shown the great potential of the membrane permeation process,[1,2] mainly because it consumes less energy compared to other traditional gas separation processes. The membrane can be composed of highly selective polymer materials, which makes the membrane process more competitive. However, it can be generally observed that highly selective polymers tend to have low permeabilities and vice versa. Thus, it is still important to develop membranes that offer low transport resistance and high selectivities (i.e., membranes exhibiting anisotropic morphology, which are composed of highly selective polymer materials). The anisotropic morphology consists of a dense skin on a support layer, which is formed by pores that gradually increase in size. The molecule transport mechanism of sorption–diffusion is normally assumed to occur in the dense skin and Knudsen diffusion or viscous flow occurs in the support layer.[3]

Despite the large number of research studies to prepare such membranes, great difficulties have been reported in obtaining a skin thickness reduction without a loss in selectivity.

Correspondence to: C. P. Borges (cristiano@peq.coppe.ufrj.br).

Contract grant sponsor: CNPq/PADCT.

Journal of Applied Polymer Science, Vol. 83, 2022–2034 (2002)

DOI 10.1002/app.10159

Fritzsche et al. used Lewis acid–base (LAB) complexes to prepare polysulfone (PSF) hollow fibers for gas separation applications.[4–9] According to these authors, the polymer solution that contains these complexes allows a higher additive content than that usually accepted in traditional solvent/nonsolvent mixtures.

When these polymer solutions are immersed in a precipitation bath composed of a nonsolvent that presents a high dieletric constant (e.g., water), a fast complex dissociation is promoted that leads to the polymer precipitation. According to Fritzsche et al. the velocity of the phase separation is higher, inhibiting compacting and conformational rearrangement of the polymer molecules. This would enhance free volume in the effective separating layer. When varying the solvent for some PSF solutions, there appeared to be a trend for the O_2 permeability to increase with the solution viscosity and solvent molecular size. The authors suggest an apparent relationship between the solvent molecule size and free volume and the permeability of the resultant membranes. When the propionic acid (PA)/*N*-methyl-2-pyrrolidone (NMP) molar ratio increased, the O_2 permeability did also whereas the O_2/N_2 selectivity stayed rather constant.[7] However, in the case of He/N_2, when increasing the PA/NMP molar ratio, the selectivity increased and the He permeability diminished.[5] Besides the solvent molecule size, these results are a clear indication that other factors may also affect the free volume and permeability of the membrane. In order to gain new insights into membrane formation when LABs are present in a polymer solution, more investigation is required.

The present work considers thermodynamic and kinetics factors to analyze the membrane morphology and permeability by investigating the influence of LAB complexes in a polymer solution. A dicarboxylic acid and homologous series of monocarboxylic acids were selected (Lewis acids) to form complexes with NMP (Lewis base). Flat poly(ether sulfone) (PES) membranes were obtained by immersion–precipitation using water as a nonsolvent because of its high dielectric constant. The membranes were characterized by scanning electron microscopy and gas permeation experiments.

EXPERIMENTAL

Flat anisotropic membranes were prepared using PES (Ultrason E6020, BASF) as the polymer.

Table I Polymer Solution Compositions of Investigated Systems

Polymer Solution	Acid:NMP Molar Ratio	Composition (wt %)
PES/AA/NMP	1:1	25/28.3/46.7
		30/26.4/43.6
		37/23.8/39.2
	1:2	25/17.4/57.6
		30/16.3/53.7
		37/14.6/48.3
PES/PA/NMP	1:1	25/32.1/42.9
		30/29.9/40.1
		37/26.9/36.1
	1:2	25/20.4/54.6
		30/19.0/51.0
		37/17.1/45.9
PES/CA/NMP	1:2	25/27.7/47.3
		30/25.9/44.1
		37/23.3/39.7
PES/AD/NMP	1:4	25/20.2/54.8
		30/18.9/51.1
		37/17.0/46.0

LAB complexes were formed by NMP as a solvent (Merck) and the following carboxylic acids (Rio Lab) as additives: acetic acid (AA), PA, *n*-caproic acid (CA), and adipic acid (AD). Distilled water was used as the precipitation bath. The polymer concentration varied from 25 to 37 wt % while the acid/NMP molar ratios used were 1:1, 1:2, and 1:4. Table I shows all of the compositions of the polymer solutions prepared.

In order to obtain flat membranes, the polymer solution was cast on a glass plate at room temperature (≅25°C, average relative humidity of 65%) and then immersed into the precipitation bath, which consisted of pure water or mixtures of water and NMP. The membranes were immersed in water overnight at 60°C for residual solvent extraction. The solvent exchange technique was applied by changing from water to ethanol and then to *n*-hexane and subsequently drying the membrane by solvent evaporation. Polymer solution was cast at 50°C, only when AD was present, which was due to its high viscosity. Membranes were chosen for coating with an elastomer solution of poly(dimethylsiloxane) (PDMS, 1.5 wt %) in isooctane, which were purchased from General Electric and Rio Lab, respectively. This type of coating with elastomer is applied to seal eventual defects on the membrane surface.

The polymer solutions were characterized by viscosity measurements at 25 and 45°C (LVTD

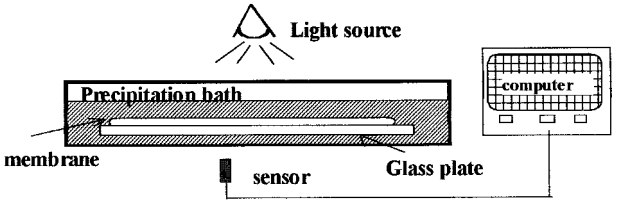

Figure 1 The light transmission apparatus.

digital viscometer, Brookfield) and by IR spectroscopy (2000-FTIR, Perkin–Elmer). The cloud point tests were also carried out by titration to determine the miscibility region. The velocity of the precipitation was evaluated by following the light transmission decay (Fig. 1) during membrane formation.

Pure gas permeation tests (CO_2 and N_2) were carried out. The gas permeation apparatus consisted of a permeation cell into which the membrane was placed and a vacuum pump for cleaning the equipment before each experiment. A calibrated pressure transducer and a bubble soap flow meter were used to measure low and high permeate fluxes, respectively.

The permeability coefficient [P/e, L^3 (STP)/L^2 θ (F/L^2), eq. (1)] and ideal selectivity [α, eq. (2)] were used as parameters for comparing membrane performances. The membrane was considered defect free when its ideal selectivity was similar to the intrinsic one of the polymer,[10] which is $\alpha_{CO_2/N_2} \cong 30$.

$$\frac{P}{e} = \frac{Q}{A \cdot \Delta P} \tag{1}$$

$$\alpha = \frac{(P/e)_i}{(P/e)_j} \tag{2}$$

where Q is the gas permeate flow rate (L^3/θ), A is the membrane permeation area (L^2), e is the membrane effective thickness (L), and ΔP is the pressure difference between the feed and permeate sides (F/L^2).

The membrane morphology was observed by scanning electron microscopy (SEM, JSM-5300, Jeol). The samples were previously coated with gold in a sputtering device.

RESULTS AND DISCUSSION

Study of Complex Formation by IR Spectroscopy

Pure solvents and their mixtures were characterized by FTIR spectroscopy to identify the presence of complexes. Figure 2 shows the IR spectra relative to the C═O absorption band of pure NMP, CA, and their mixture in a molar ratio of acid/NMP of 1:2. Besides the peaks relative to NMP and the acid, a third peak appears in the binary solution, indicating the presence of the complex. The same evidence was found in all the investigated cases. Figures 3 and 4 show the IR spectra

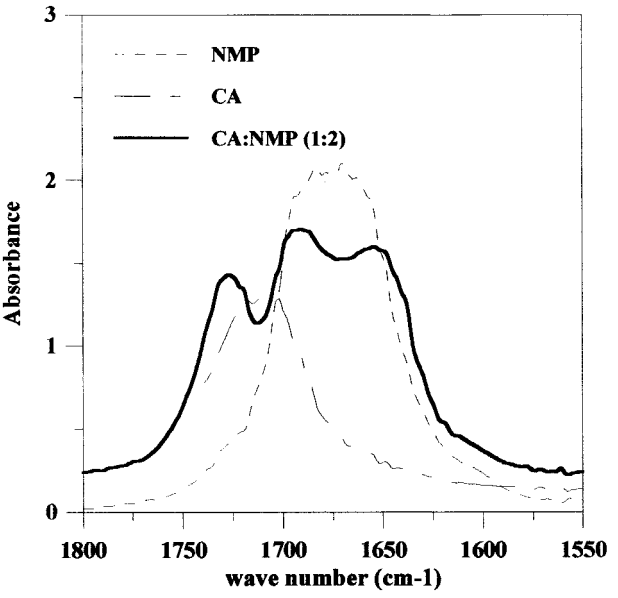

Figure 2 IR spectra relative to the C═O absorption band of pure NMP, *n*-caproic acid, and their mixture using an acid/NMP molar ratio of 1:2.

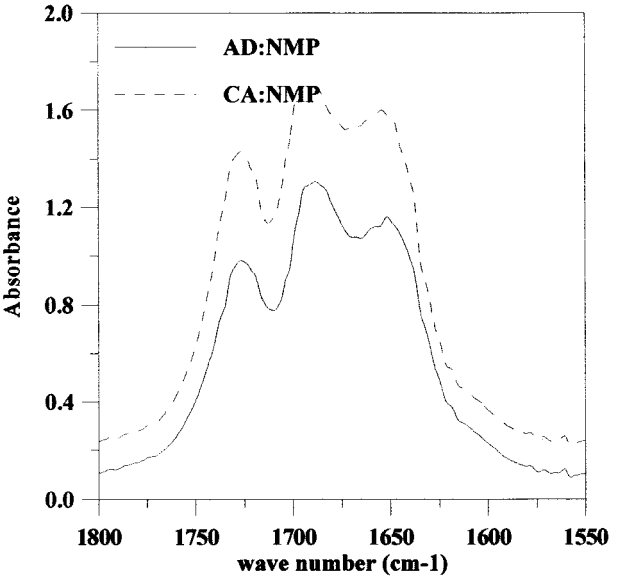

Figure 3 IR spectra relative to the C═O absorption band of all the binary acid/NMP solutions with a molar ratio of 1:2.

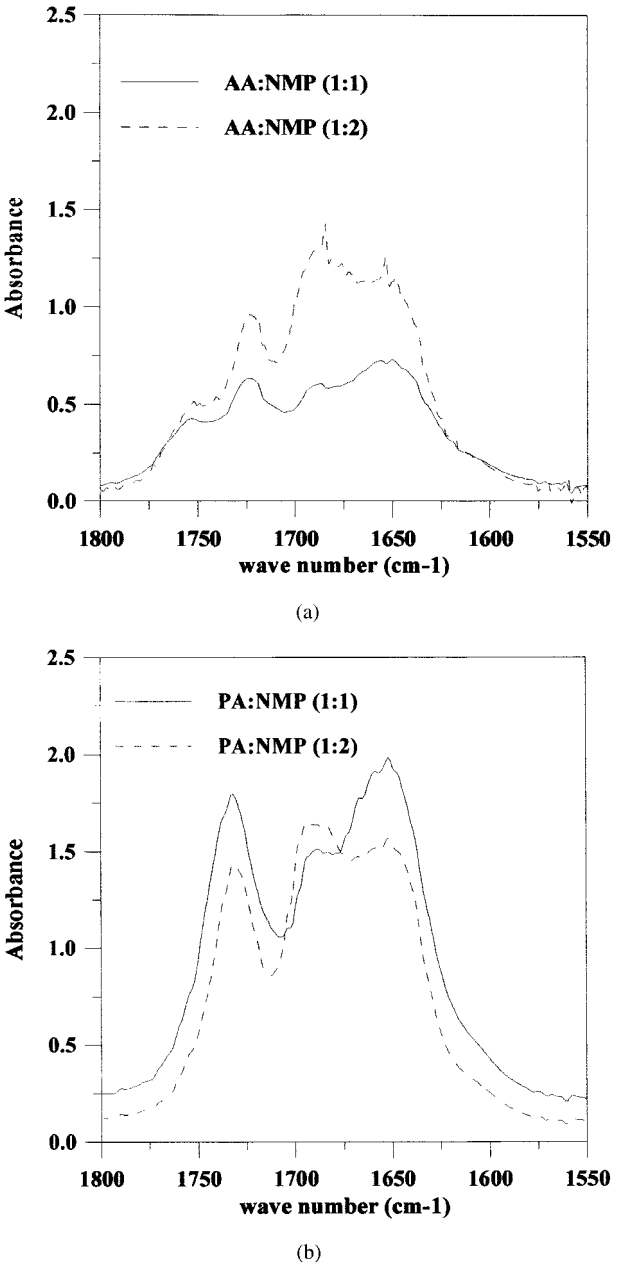

Figure 4 IR spectra relative to the C═O absorption band of the binary solutions of (a) AA/NMP with molar ratios from 1:1 to 1:2 and (b) PA/NMP with molar ratios from 1:1 to 1:2.

of all the binary acid/NMP solutions. Figure 4 shows a binary solution of AA/NMP and PA/NMP at molar ratios of 1:1 and 1:2. It can be observed that at a lower NMP concentration the NMP absorbance (wavenumber = 1685 cm^{-1}) decreases when compared to the acid (wavenumber = 1760 cm^{-1}) and complex (wavenumber = 1650 cm^{-1}) absorbances.[11] On the other hand, the absorbance ratio of the acid to the complex was constant as one may observe in Figure 4. In the molar ratio studied, these results indicate that the LAB complex formation was limited to a definite amount of solvent molecules.

Viscosity Measurements

Figure 5(a,b) shows the viscosity of the investigated polymer solutions at 25 and 45°C, respectively, as well as the PES/NMP solution (i.e., without additive). From these figures one may observe a significant increase in the viscosity values when the acids were applied as additives. The

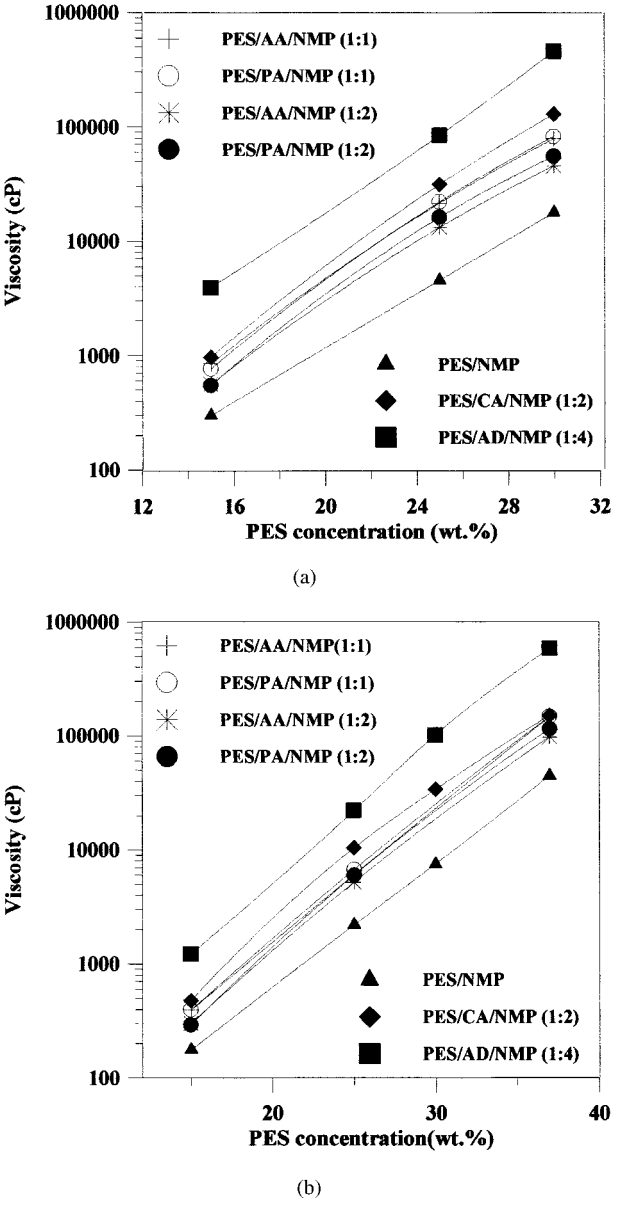

Figure 5 The viscosity of the investigated polymer solutions at (a) 25 and (b) 45°C.

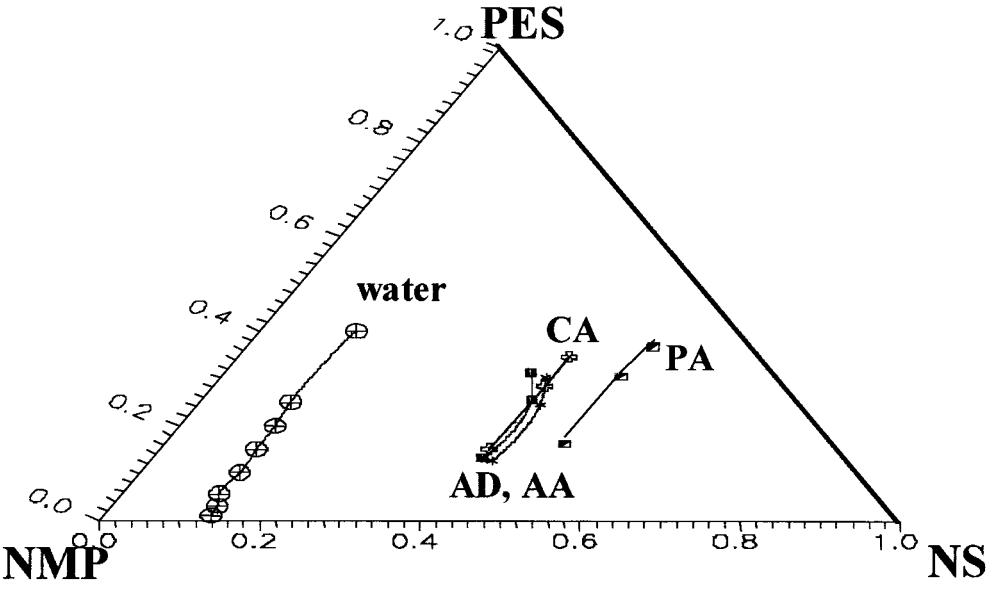

Figure 6 A ternary phase diagram of PES/additive/NMP: (✣) CA, (■) AD, (*) AA, (◩) PA, and (⊕) water.

viscosity values also increased when the acid/NMP molar ratio varied from 1:2 to 1:1. These results show the influence of the presence of complexes, considering that there are fewer free solvent molecules because of their formation. When the solutions formed by different acids are compared, one may observe that the viscosity increases with the acid chain length, indicating a better association with NMP, as well as with the polymer, due to hydrophobic interactions.

Phase Diagrams

A ternary phase diagram of PES/additive/NMP is shown in Figure 6. The solutions containing acids as additives present a larger miscibility gap compared to water as an additive (PES/water/NMP data from Zeman and Tkacik[12]), which indicates greater affinity the PES–acids. Comparing the solutions with different acids, there are two different effects caused by increasing the carbon content (—CH_2—) in the acid. There was a larger miscibility gap with PA than with AA, which was probably due to a higher polymer–acid affinity. On the other hand, when comparing AA to CA the binodal shifts toward the polymer–solvent axis, decreasing the miscibility gap. These opposing effects may be attributed to the capacity to form an acid/NMP complex. A measure of the electrophilic and nucleophilic properties of Lewis acid and base solvents can be given by the Gutmann[13,14] donor (DN, FL/mol) and acceptor (AN, FL/mol) numbers, respectively. According to literature data, the acid strength seems to decrease with the chain length increase, which is indicated by a lower donor number (e.g., for AA the AN = 52.9, for PA the AN = 49.1, and for isobutyric acid the AN = 47 kcal/mol). Because NMP is a weak base (DN = 17.3 kcal/mol), it will favorably interact with the weaker acid, like the longer acid chain length CA in the monocarboxylic series studied in the present work. It appears that the interaction between CA and NMP is stronger than between the polymer and acid. Therefore, in the CA/NMP/PES system the miscibility gap diminishes. In AD the presence of two dicarboxylic acid groups makes it stronger than CA. This reduces its interaction with NMP and, consequently, increases the miscibility gap. On the other hand, the polymer–additive interaction is also reduced. Consequently, the binodal is located between the investigated acids.

These results show that the miscibility gap depends not only on the hydrophobic character of the acid but also on its capacity of forming complexes with the solvent and therefore the amount of NMP molecules available.

Figure 7 shows pseudoternary diagrams using the sum of the solvent and additive as one single component, because they are forming a complex in the solution. The results for AA and PA for two different acid/NMP molar ratios are shown in Figure 7(a,b), respectively. It can be seen that the miscibility gap increases considerably from the 1:1 to 1:2 (acid/NMP) molar ratio, which occurs

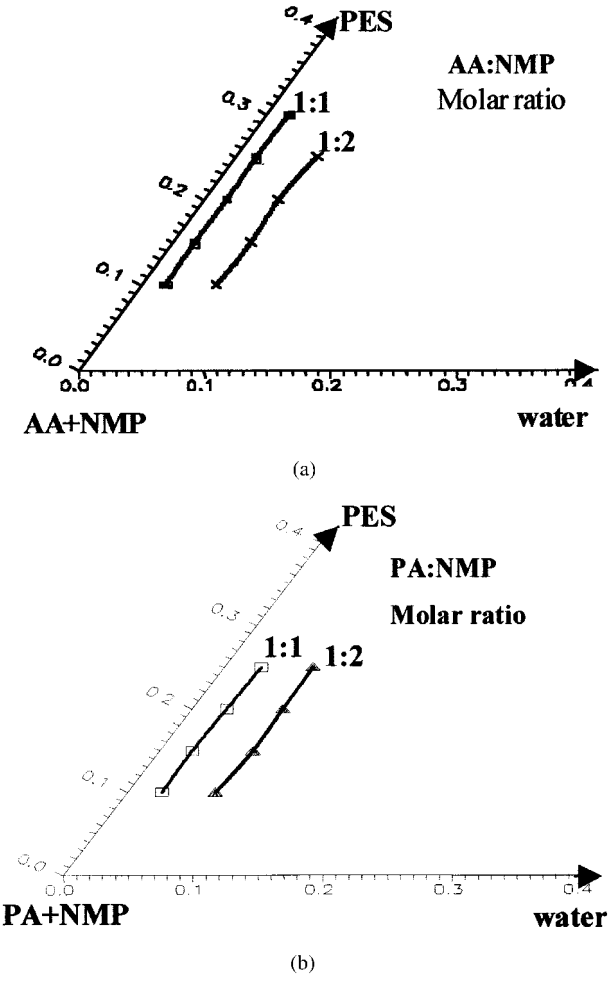

Figure 7 Pseudoternary diagrams of (a) PES/AA/NMP with AA/NMP molar ratios from 1:1 to 1:2 and (b) PES/PA/NMP with PA/NMP molar ratios from 1:1 to 1:2.

due to a higher content of solvent molecules available in the latter. When the different acids are compared at the same molar ratio (Fig. 8), the same sequence of binodal shifts was obtained in the ternary phase diagram. This result reinforces the arguments of the previous analysis and indicates that it is adequate to represent the phase diagram by using the acid–base molar ratio as a parameter.

Light Transmission Measurements

Figure 9 shows the light transmission during precipitation when the polymer solution films cast on a glass plate (25 wt % PES) were exposed to the environment for a long period of time. It can be seen that the demixing onsets of the solutions were quite different. The difference in the precipitation velocity between the solutions composed of AA and PA at a 1:1 acid/NMP molar ratio is presented in a larger scale for the first 5 min of the experiments in Figure 10. From these figures it is observed that the demixing onset sequence is in agreement with the binodal position in the phase diagrams for all the solutions but AD. This shows the influence of the miscibility gap on the velocity of precipitation, which was mainly promoted by water vapor sorption from the environment. In the solution composed of AD, the longer onset observed also indicates the influence of the high viscosity value of the solution, which inhibits water inflow from the environment.

When the polymer solution demixing occurred because of immersion into a precipitation bath, varying its composition, there was no considerable difference in the light transmission (Fig. 11). This is evidence that the dissociation rate by wa-

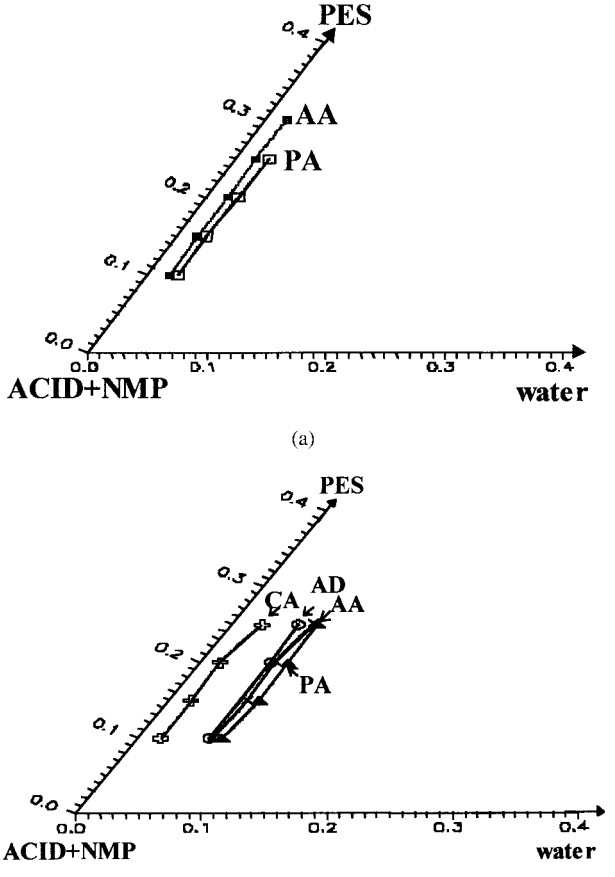

Figure 8 Pseudoternary diagrams of (a) PES/AA/NMP and PES/PA/NMP at an acid/NMP molar ratio of 1:1; (b) PES/AA/NMP, PES/PA/NMP, and PES/CA/NMP at an acid/NMP molar ratio of 1:2; and PES/AD/NMP at an acid/NMP molar ratio of 1:4.

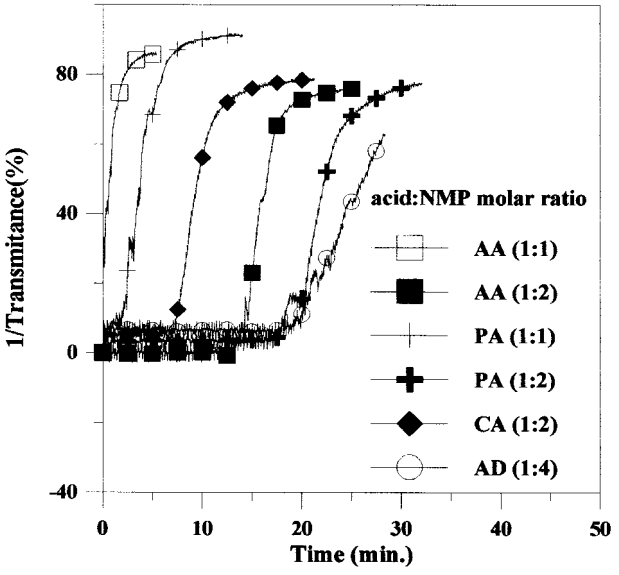

Figure 9 The light transmission decay when the polymer solutions (25 wt % PES) were exposed to the environment for a long period of time.

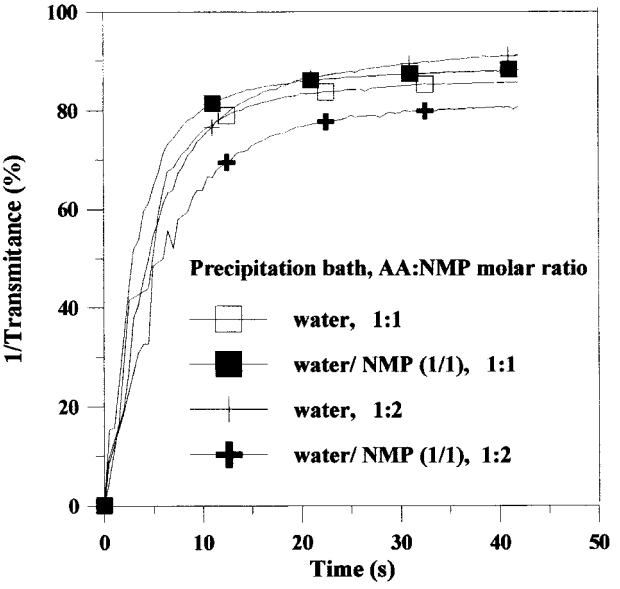

Figure 11 The light transmission decay of PES/AA/NMP with various precipitation baths and compositions and AA/NMP molar ratios.

ter was fast enough to characterize an instantaneous precipitation. In the AD the velocity of precipitation became slower as the polymer concentration increased (Fig. 12). However, once more, the difference is not significant when varying the precipitation bath composition. These results once again show the influence of the viscosity on mass transfer between the precipitation bath and the polymer solution. Under all conditions, there was no observed light transmission decay during the 2 h when the solutions were immersed into a precipitation bath consisting of 1/9 (w/w) water/NMP. This indicates that reducing the amount of water in the precipitation bath inhibits complete dissociation and, consequently, solution precipita-

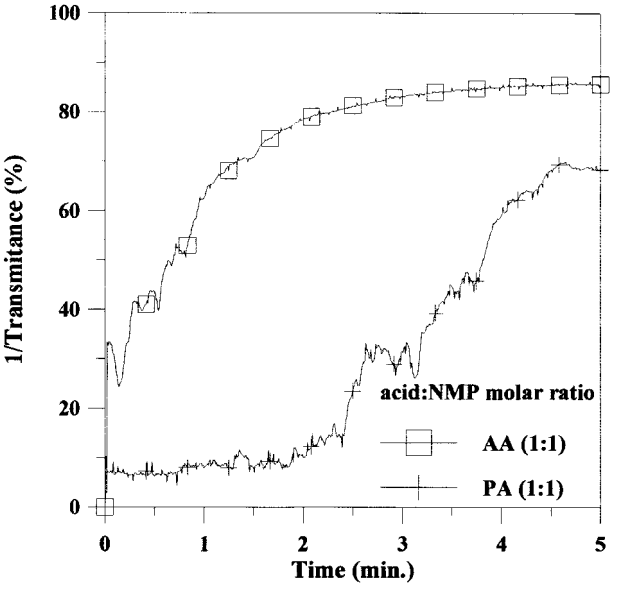

Figure 10 The light transmission decay of PES/AA/NMP when the PES/acid/NMP acids (AA and PA, 25 wt % PES) were exposed to the environment for a long period of time.

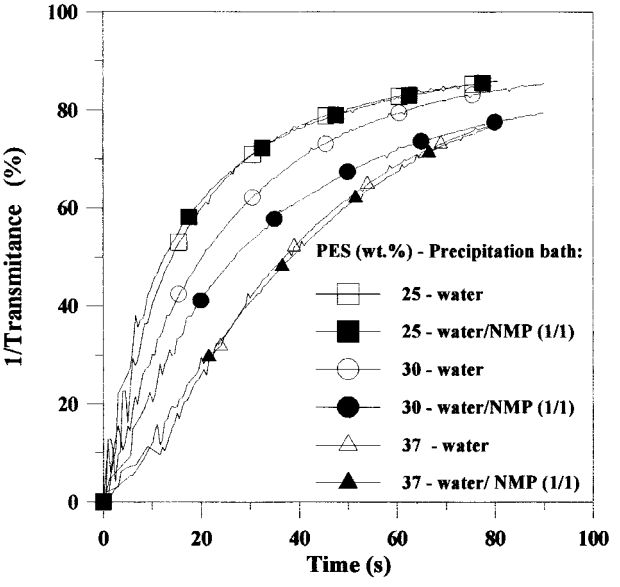

Figure 12 The light transmission decay of PES/AD/NMP with various precipitation baths and PES compositions.

Table II Gas Permeation Results of Membranes Obtained from PES/Acid/NMP Solutions with 25 wt % = PES

Acid (Molar Ratio)	Precipitation Bath Water/ NMP (w/w)	P/e CO_2 (GPU)	α CO_2/N_2
CA (1:2)	1/0	624.0	0.8
	1/1	78.3	0.7
AD (1:4)	1/0	51.7	0.8
	1/1	3.4	1.8
AA (1:2)	1/0	6.2	1.7
	1/1	5.5	0.8
PA (1:2)	1/0	3.8	1.6
	1/1	6.3	0.7

1 gas permeation unit (GPU) = 10^{-6} cm^3/cm^2 s cmHg.

tion. NMP outflow was also not favored because of its high concentration in the precipitation bath, which also did not favor the complex dissociation.

Gas Permeation Tests

Table II shows the pure gas (CO_2 and N_2) permeation results of the membranes obtained from PES/acid/NMP solutions with 25 wt % PES, and acid/NMP molar ratios of 1:2 (AA, PA, CA) and 1:4 (AD).

It can be observed for the membranes obtained by using water as a precipitation bath that the permeability coefficients followed the binodal shift observed in the phase diagram: a larger miscibility gap for the polymer solution resulted in a lower permeability coefficient. However, one may also expect a dependence of the permeability coefficient on the precipitation velocity of the polymer solution. Faster demixing usually leads to a more open porous membrane and subsequent higher permeability coefficients. The precipitation velocity depends on the mass exchange rate between the precipitation bath and the polymer solution, as well as on the binodal location. In other words, as the binodal comes closer to polymer–solvent axis, more nonsolvent is required in the polymer solution to dissociate the complex and form nuclei of the polymer lean phase, which promotes their growth. Thus, when water was used in the precipitation bath one may expect a high mass transfer rate and a consequent high dissociation rate. Thus, the importance of the binodal location increases, which favors liquid–liquid demixing and the nucleation process.

The importance of binodal shift to the permeability was smaller when water/NMP (1/1, w/w) was used as the precipitation bath. In this case a reduction in the mass transfer rate is expected, as well as in the complex dissociation and precipitation rates; consequently, there are smaller permeability coefficients. This can be observed in Table II for all investigated solutions, except the one with PA. Another observation on the membranes obtained using this precipitation bath is that the permeability sequence is not in agreement with the binodal shift in the phase diagram. One hypothesis to explain these results is the competition between liquid–liquid demixing and the vitrification phenomenon in the region close to the interface of the bath–polymer solution. Indeed, the vitrification phenomenon may be favored when a reduction in the dissociation rate of the complex occurs because of a decrease in the mass transfer gradients. This effect reduces the influence of the binodal location and makes its correlation with the permeability coefficient more difficult.

The results presented in Table III (PES/acid/NMP solutions, 25 wt % PES, acid/NMP molar ratio of 1:1 for AA and PA) show that the permeability coefficients were also higher for the membranes obtained using water as the precipitation bath. This reinforces the previous analysis. In the water/NMP (1/1, w/w) precipitation bath the vitrification phenomenon in the region close to the interface of the bath–polymer solution again seems to be prior to liquid–liquid demixing due to a reduction in the mass transfer rate.

Comparing the results obtained with AA and PA (Tables II, III) with molar ratios of 1:2 to 1:1 and using water as the precipitation bath, one may observe that the permeability coefficients of the membranes were higher when the molar ratio applied was 1:1. This result is also in agreement with the binodal location in the phase diagram. Once again, the difference is not so expressive when water/NMP (1/1) was used as the precipitation bath.

Table III Gas Permeation Results of Membranes Obtained from PES/Acid/NMP Solutions with 25 wt % PES

Acid	Precipitation Bath Water/ NMP (w/w)	P/e CO_2 (GPU)	α CO_2/N_2
AA (1:1)	1/0	60.4	0.8
	1/1	6.0	0.9
PA (1:1)	1/0	23.3	0.7
	1/1	7.2	1.1

Table IV Gas Permeation Results of Membranes Obtained from PES/Acid/NMP Solutions with 30–37 wt % PES and Acid:NMP Molar Ratios of 1:2 for AA, PA, and CA and 1:4 for AD

		P/e CO_2 (GPU)		α CO_2/N_2	
Acid	Precipitation Bath Water/NMP (w/w)	30% PES	37% PES	30% PES	37% PES
CA	1/0	1.9	2.7	1.7	1.3
	1/1	8.7	0.8	1.3	14.4
AD	1/0	5.4	1.3	1.1	6.1
	1/1	6.9	1.5	1.2	1.7
AA	1/0	3.1	1.3	2.2	18.3
	1/1	2.5	0.3	1.7	19.1
PA	1/0	4.6	1.5	1.2	2.8
	1/1	3.4	2.7	0.9	6.1

Tables IV and V show the results obtained with the solutions with a higher polymer concentration. In these systems, because of higher solution viscosity, a reduction in the mass transfer between the precipitation bath and the polymer solution occurs. In these conditions the complex dissociation effect becomes secondary: the membrane structure is determined mainly because of viscous effects (e.g., vitrification) resulting from the high polymer concentration. As observed previously, when these effects are favored, the difference in the permeability coefficient is not meaningful. One may also observe that in all these conditions selective membranes were obtained (i.e., the sorption–diffusion mechanism may be applied), indicating that a dense top layer is present.

In comparing different bath compositions it can be seen in Table V that the obtained membranes present the same permeability tendency as verified previously for the solutions with 25 wt % PES, although this was not observed for all investigated solutions when the molar ratio applied was 1:2, as presented in Table IV. The proximity of the region where the viscous effects are predominant makes complete comprehension of the results difficult. However, they may be attributed to the difference in the miscibility gap and dissociation rate with different acids.

Because of the highest selective values obtained with the membranes prepared from PES/AA/NMP/water, these membranes were coated with an elastomer solution (1.5 wt % PDMS in isooctane). After coating the selectivity values strongly increased (Table VI), which indicated a higher contribution to the transport by the sorption–diffusion mechanism; thus, the presence of dense top layers is verified. One may also observe that the permeability coefficient of the coated membranes was higher when the AA/NMP molar ratio was 1:1 and the polymer concentration was lower, indicating higher surface porosity and lower transport resistance. This is probably due to the presence of a higher concentration of AA molecules at the complex dissociation, promoting a support for the higher porosity. The membranes obtained by using 37 wt % PES presented higher selectivity than is intrinsic to the polymer, indicating a change in the molecular packing of the polymer solutions composed of the LAB complex.

Table V Gas Permeation Results of Membranes Obtained from PES/Acid/NMP Solutions with 30–37 wt % PES and Acid:NMP Molar Ratio of 1:1 for AA and PA

		P/e CO_2 (GPU)		α CO_2/N_2	
Acid	Precipitation Bath Water/NMP (w/w)	30% PES	37% PES	30% PES	37% PES
AA	1/0	2.9	1.7	0.6	7.2
	1/1	1.2	0.3	0.5	17.6
PA	1/0	—	6.2	1.1	3.4
	1/1	3.1	1.9	1.9	4.0

— Not measured.

Table VI Gas Permeation Results of Membranes Prepared from PES/AA/NMP/Water

PES Concn (wt %)	AA:NMP Molar Ratio	*P/e* CO_2 (GPU)	α^* CO_2/N_2
25	1:1	9.6	10.0
	1:2	3.9	9.3
30	1:1	2.0	9.5
	1:2	1.7	12.7
37	1:1	1.7	29.8
	1:2	0.7	41.1

* These membranes were coated with an elastomer solution (1.5 wt % PDMS in isoctane).

Morphology of Membranes

In all investigated cases, when NMP was added to the precipitation bath, the membranes presented a reduction in macropore formation, as can be observed in the SEM photomicrographs presented in Figure 13 for the membranes formed by PES/AA/NMP. As already observed in other studies,[15] this result indicates that, in the initial precipitation instant, the mass transfer between the polymer solution and precipitation bath is reduced. The main consequence is a reduction of the mass transfer resistance and inhibition of nuclei growth in the sublayer.

The PES concentration also influenced macropore formation. When the polymer solution with PA as the additive was used (PA:NMP molar ratio = 1:1), which increased the PES concentration, the resulting membranes presented an oscillatory behavior,[15,16] as can be seen in Figure 14. An increase of the polymer concentration leads to a higher mass transfer resistance between the polymer solution and the precipitation bath, as well as a reduction of the miscibility gap, promoting different time intervals for nuclei growth. According to this assumption, by increasing the polymer concentration from 25 to 30 wt % in the latter, the mass transfer resistance close to the top layer keeps the sublayer stable for a longer time, which allows the nuclei to grow. When the polymer concentration increases to 37 wt %, the reduction in the miscibility gap becomes the prior effect, accelerating phase demixing in the sublayer and inhibiting macropore growth.

When a PA/NMP molar ratio of 1:2 was applied, there was an absence of macropores. In this molar ratio the system presents a larger miscibility gap, which may decrease the velocity of precipitation. However, this probably occurs mainly in the top layer; thus, water is allowed to reach the inner layers, promoting complex dissociation and, consequently, faster precipitation that inhibits its macropore formation. This is effect is similar to that observed when NMP was present in the precipitation bath. This macropore absence may increase membrane transport resistance, as verified in the gas permeation experiments.

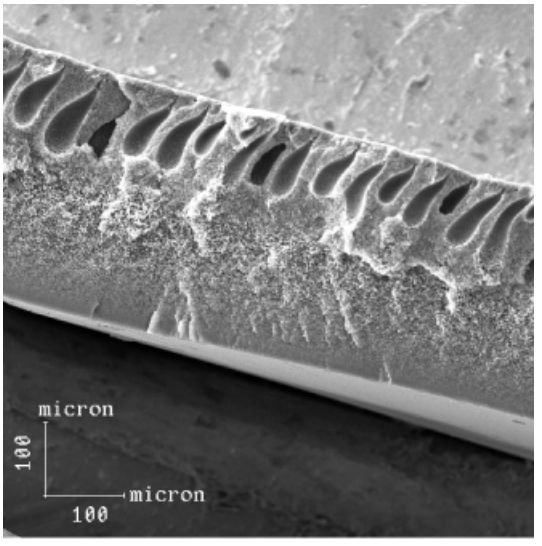

(a)

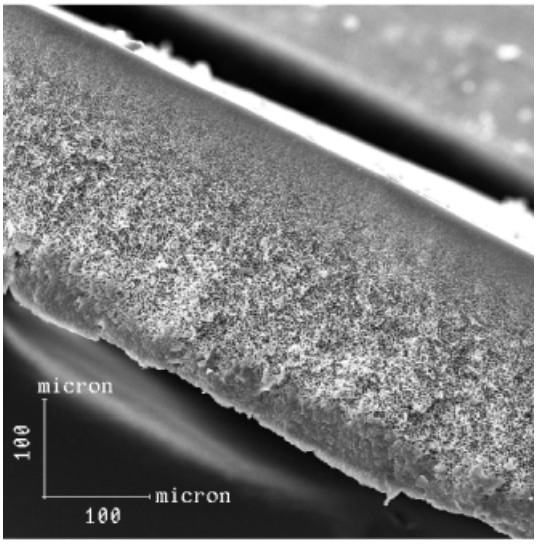

(b)

Figure 13 SEM photomicrographs of the membranes formed by PES/AA/NMP (30/26.4/43.6 wt %) at an AA/NMP molar ratio of 1:1. The precipitation bath is composed of water/NMP with compositions (w/w) of (a) 1/0 and (b) 1/1.

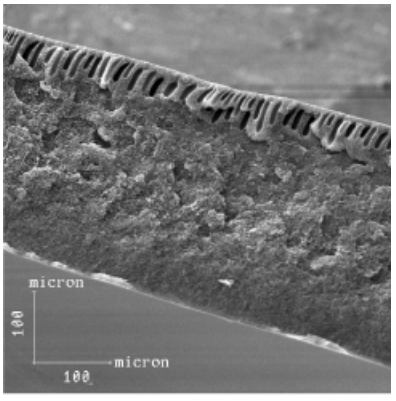

(a)

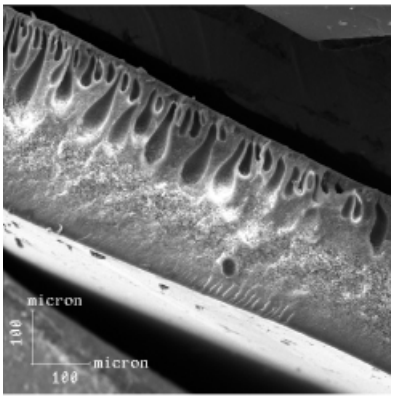

(b)

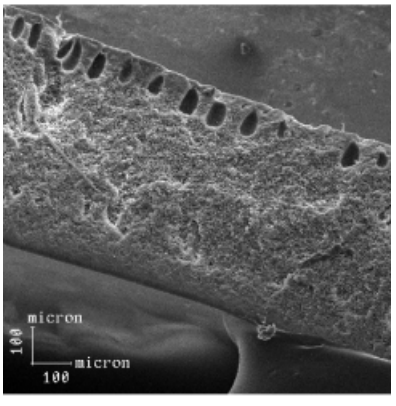

(c)

Figure 14 SEM photomicrographs of the membranes formed by PES/PA/NMP at a PA/NMP molar ratio of 1:1. The precipitation bath is water and the PES compositions (wt %) are (a) 25, (b) 30, and (c) 37.

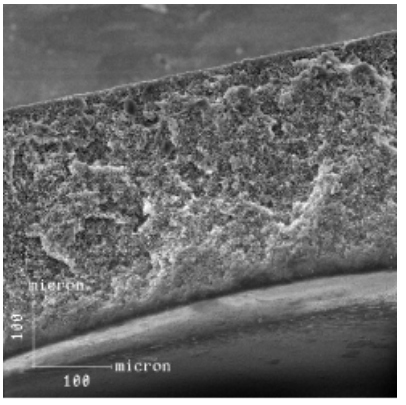

(a)

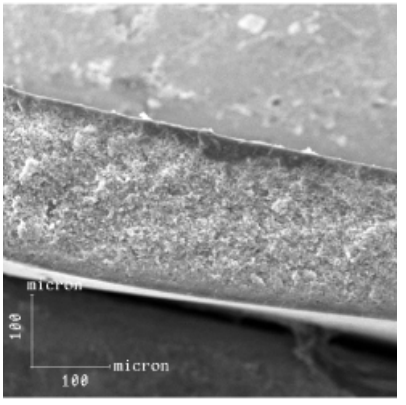

(b)

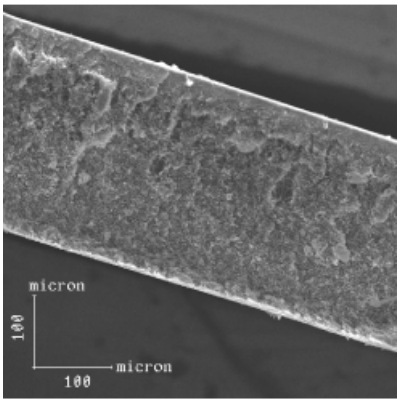

(c)

Figure 15 SEM photomicrographs of the membranes formed by PES/PA/NMP at a PA/NMP molar ratio of 1:2. The precipitation bath is water and the PES compositions (wt %) are (a) 25, (b) 30, and (c) 37.

The molar ratio and polymer concentration effects when AA was used as an additive are shown in Figures 16 and 17. The same behavior described for PA was observed with an AA/NMP molar ratio of 1:1. However, with a molar ratio of 1:2 (Fig. 17) the macropores are clearly observed.

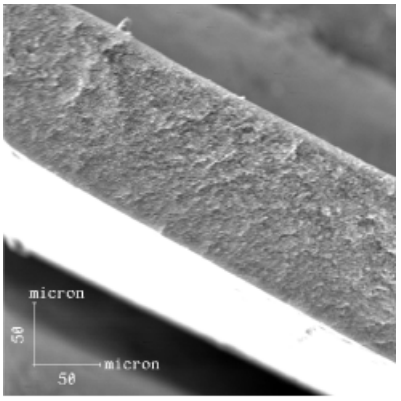

(a)

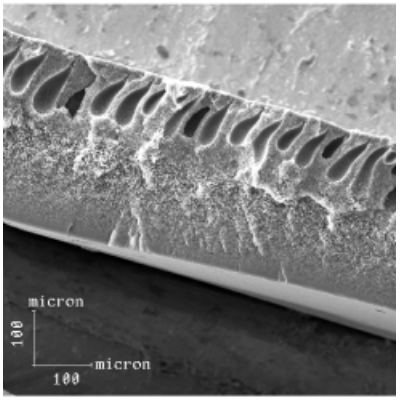

(b)

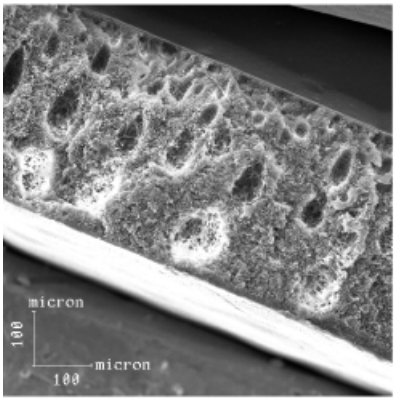

(c)

Figure 16 SEM photomicrographs of the membranes formed by PES/AA/NMP at an AA/NMP molar ratio of 1:1. The precipitation bath is water and the PES compositions (wt %) are (a) 25, (b) 30, and (c) 37.

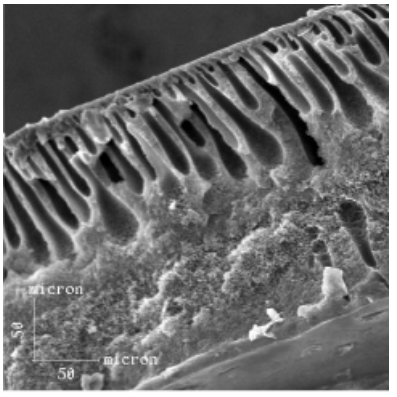

(a)

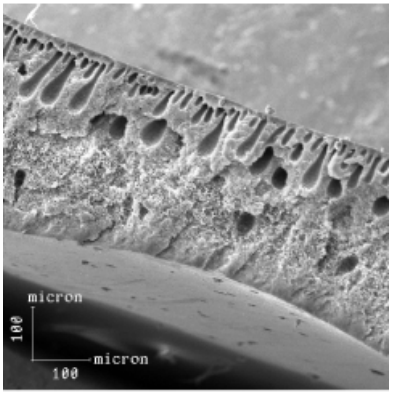

(b)

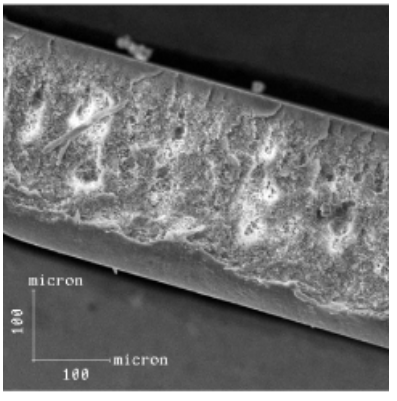

(c)

Figure 17 SEM photomicrographs of the membranes formed by PES/AA/NMP at an AA/NMP molar ratio of 1:2. The precipitation bath is water and the PES compositions (wt %) are (a) 25, (b) 30, and (c) 37.

Increasing the polymer concentration seems to reduce macropore formation, indicating that the miscibility gap was the major effect in this case.

In the solutions composed of AA the velocity of precipitation is fast enough to increase the mass transfer resistance near the interface between the

polymer solution and the precipitation bath, promoting delay in the sublayer and, as discussed before, macropore formation. This result is in agreement with the analysis of the system composed of PA with the same molar ratio, because the latter presents a larger miscibility gap.

In the solutions composed of AD and CA (acid/NMP molar ratios of 1:4 and 1:2, respectively) the results and analysis are similar to the system composed of 1:1 PA/NMP. It is appropriate to emphasize that the systems composed of AD and CA present miscibility gaps similar to AA and PA when the acid/NMP ratio is 1:1.

CONCLUSIONS

The results showed that the presence of LAB complexes must be taken into consideration to predict membrane properties. To do so, the use of the molar ratio of the acid–base pair proved to be a good parameter for analysis, because it showed that the results of the analysis of different characterizations (thermodynamic and kinetic factors) were clearly connected. However, we must emphasize the importance of the dissociation rate of the complexes, which depends on the acid–base strength (i.e., complex stability). In sum, the number of solvent molecules available (base component), which are defined by the molar ratio applied and the acid–base strength, as defined by the component characteristics (physicochemical properties of size and affinity), clearly influenced the miscibility region, viscosity, and velocity of precipitation, which determine the membrane morphology, permeability, and selectivity. Another important effect observed is that the membranes obtained with 37 wt % PES and AA/NMP as the LABs presented higher selectivity than the polymer intrinsic value. This probably indicates molecular packing of the polymer solutions composed of LAB.

The authors would like to thank CAPES and CNPq for the first author's (C.C.P.) scholarship during her D.Sc. thesis and CNPq/PADCT for financial support.

REFERENCES

1. Ghosal, K.; Freeman, B. D. Polym Adv Technol 1994, 5, 673.
2. Pinnau, I. Polym Adv Technol 1994, 5, 733.
3. Mulder, M. H. V. Basic Principles of Membrane Technology; Kluwer Academic: Amsterdam, 1991.
4. Fritzsche, A. K.; Kesting, R. E.; Murphy, M. K. J Membr Sci 1989, 46, 135.
5. Fritzsche, A. K.; Cruse, C. A.; Kesting, R. E.; Murphy, M. K. J Appl Polym Sci 1990, 39, 1949.
6. Fritzsche, A. K.; Armbruster, B. L.; Fraundorf, P. B.; Pellegrin, C. J. J Appl Polym Sci 1990, 39, 1915.
7. Kesting, R. E.; Fritzsche, A. K.; Murphy, M. K.; Cruse, C. A.; Handermann, A. C.; Malon, R. F.; Moore, M. D. J Appl Polym Sci 1990, 40, 1557.
8. Kesting, R. E.; Fritzsche, A. K.; Murphy, M. K.; Cruse, C. A.; Moore, M. D. J Appl Polym Sci 1990, 40, 1575.
9. Fritzsche, A. K.; Cruse, C. A.; Kesting, R. E.; Murphy, M. K. J Appl Polym Sci 1990, 40, 19.
10. Pereira, C. C.; Habert, A. C.; Nobrega, R.; Borges, C. P. In Proceedings of II Congresso Ibero Americano em Ciência e Tecnologia de Membranas—CITEM; Habert, A. C.; Nobrega, R.; Borges, C. P., Eds.; COPPE/UFRJ: Rio de Janeiro, 1994; p 292.
11. Silverstein, R. M.; Bassler, G. C. Spectrometric Identification of Organic Compounds, 2nd ed.; Wiley: New York, 1967.
12. Zeman, L.; Tkacik, G. J Membr Sci 1988, 36, 119.
13. Mayer, U. Pure Appl Chem 1979, 51, 1697.
14. Reichardt, C. Solvent Effects in Organic Chemistry; Verlag Chemie: New York, 1978.
15. Machado, P. S. T.; Habert, A. C.; Borges, C. P. J Membr Sci 1999, 155, 171.
16. Pereira, C. C. D.Sc. thesis, COPPE/Federal University of Rio de Janeiro, 1999.